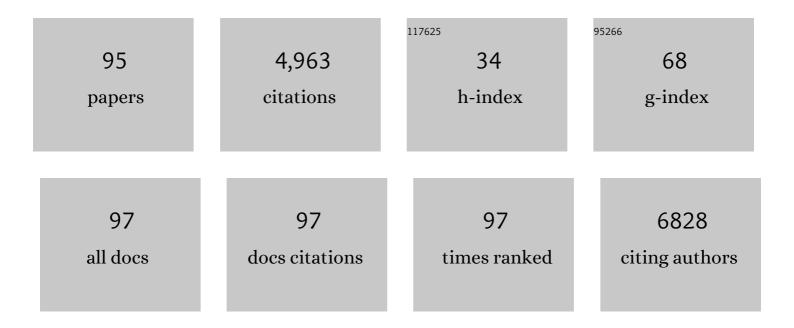
List of Publications by Year in descending order

Source: https://exaly.com/author-pdf/669250/publications.pdf Version: 2024-02-01



DONC PIP KIM

#	Article	IF	CITATIONS
1	Visibly Clear Radiative Cooling Metamaterials for Enhanced Thermal Management in Solar Cells and Windows. Advanced Functional Materials, 2022, 32, 2105882.	14.9	51
2	Optical investigation of cryogenic frost formation under forced convection. Applied Thermal Engineering, 2022, 202, 117887.	6.0	10
3	Enhanced thermal performance of phase change material-integrated fin-type heat sinks for high power electronics cooling. International Journal of Heat and Mass Transfer, 2022, 184, 122257.	4.8	21
4	Investigating the role of metals loaded on nitrogen-doped carbon-nanotube electrodes in electroenzymatic alcohol dehydrogenation. Applied Catalysis B: Environmental, 2022, 307, 121195.	20.2	11
5	Biodegradable silicon nanoneedles for ocular drug delivery. Science Advances, 2022, 8, eabn1772.	10.3	31
6	Frost formation from general-low to ultra-low temperatures: A review. International Journal of Heat and Mass Transfer, 2022, 195, 123164.	4.8	12
7	Modeling of frost growth and fog generation at ultra-low temperatures. International Journal of Heat and Mass Transfer, 2021, 166, 120741.	4.8	9
8	Acetogenic bacteria utilize light-driven electrons as an energy source for autotrophic growth. Proceedings of the National Academy of Sciences of the United States of America, 2021, 118, .	7.1	47
9	Controlled Integration of Interconnected Pores under Polymeric Surfaces for Low Adhesion and Antiscaling Performance. ACS Applied Materials & Interfaces, 2021, 13, 13684-13692.	8.0	10
10	Frost growth mechanism and its behavior under ultra-low temperature conditions. International Journal of Heat and Mass Transfer, 2021, 169, 120941.	4.8	28
11	Replicable Quasi-Three-Dimensional Plasmonic Nanoantennas for Infrared Bandpass Filtering. ACS Applied Materials & Interfaces, 2021, 13, 24024-24031.	8.0	4
12	Rapid custom prototyping of soft poroelastic biosensor for simultaneous epicardial recording and imaging. Nature Communications, 2021, 12, 3710.	12.8	24
13	Power optimization for defrosting heaters in household refrigerators to reduce energy conversion and Management, 2021, 237, 114127.	9.2	7
14	Genome-Scale Analysis of Acetobacterium woodii Identifies Translational Regulation of Acetogenesis. MSystems, 2021, 6, e0069621.	3.8	8
15	High quality GaN tetrapodal structures hetero-integrated on 3D Si surfaces. Applied Surface Science, 2021, 565, 150584.	6.1	1
16	Frost layer growth behavior on ultra-low temperature surface with a superhydrophobic coating. International Communications in Heat and Mass Transfer, 2021, 128, 105641.	5.6	9
17	Numerical modeling and experimental validation of a phase change material-based compact cascade cooling system for enhanced thermal management. Applied Thermal Engineering, 2020, 164, 114470.	6.0	19
18	Cooling performance and space efficiency improvement based on heat sink arrangement for power conversion electronics. Applied Thermal Engineering, 2020, 164, 114458.	6.0	11

#	Article	IF	CITATIONS
19	Enhanced thermal performance of lithium nitrate phase change material by porous copper oxide nanowires integrated on folded meshes for high temperature heat storage. Chemical Engineering Journal, 2020, 391, 123613.	12.7	13
20	Layer-by-layer assembled phase change composite with paraffin for heat spreader with enhanced cooling capacity. Energy Conversion and Management, 2020, 204, 112287.	9.2	6
21	Frost modeling under cryogenic conditions. International Journal of Heat and Mass Transfer, 2020, 161, 120250.	4.8	25
22	Bactericidal Lubricating Synthetic Materials for Three-Dimensional Additive Assembly with Controlled Mechanical Properties. ACS Applied Materials & Interfaces, 2020, 12, 26464-26475.	8.0	3
23	Bioresorbable, Miniaturized Porous Silicon Needles on a Flexible Water-Soluble Backing for Unobtrusive, Sustained Delivery of Chemotherapy. ACS Nano, 2020, 14, 7227-7236.	14.6	50
24	3D Printed Bioresponsive Devices with Selective Permeability Inspired by Eggshell Membrane for Effective Biochemical Conversion. ACS Applied Materials & Interfaces, 2020, 12, 30112-30119.	8.0	5
25	Evaluation of thermomechanical behaviors of UO2-5 vol% Mo nuclear fuel pellets with sandwiched configuration. Journal of Nuclear Materials, 2020, 539, 152295.	2.7	6
26	Enhanced water collection of bio-inspired functional surfaces in high-speed flow for high performance demister. Desalination, 2020, 479, 114314.	8.2	14
27	Adaptive Laboratory Evolution of Eubacterium limosum ATCC 8486 on Carbon Monoxide. Frontiers in Microbiology, 2020, 11, 402.	3.5	44
28	Functional cooperation of the glycine synthase-reductase and Wood–Ljungdahl pathways for autotrophic growth of <i>Clostridium drakei</i> . Proceedings of the National Academy of Sciences of the United States of America, 2020, 117, 7516-7523.	7.1	88
29	Recent progress on developing anti-frosting and anti-fouling functional surfaces for air source heat pumps. Energy and Buildings, 2020, 223, 110139.	6.7	20
30	Genome Engineering of <i>Eubacterium limosum</i> Using Expanded Genetic Tools and the CRISPR-Cas9 System. ACS Synthetic Biology, 2019, 8, 2059-2068.	3.8	38
31	Frost layer growth behavior under cryogenic conditions. Applied Thermal Engineering, 2019, 163, 114333.	6.0	33
32	Sensor-Instrumented Scaffold Integrated with Microporous Spongelike Ultrabuoy for Long-Term 3D Mapping of Cellular Behaviors and Functions. ACS Nano, 2019, 13, 7898-7904.	14.6	8
33	Direct growth of hierarchical nanoneedle arrays with branched nanotubes from titanium foil with excellent anti-corrosion and superhydrophilicity. Chemical Engineering Journal, 2019, 372, 616-623.	12.7	6
34	Hierarchical Macroporous Particles for Efficient Whole-Cell Immobilization: Application in Bioconversion of Greenhouse Gases to Methanol. ACS Applied Materials & Interfaces, 2019, 11, 18968-18977.	8.0	57
35	Numerical and experimental investigation on thermal expansion of UO2-5 vol% Mo microcell pellet for qualitative comparison to UO2 pellet. Journal of Nuclear Materials, 2019, 518, 342-349.	2.7	9
36	SiO2 microparticles with carbon nanotube-derived mesopores as an efficient support for enzyme immobilization. Chemical Engineering Journal, 2019, 359, 1252-1264.	12.7	154

#	Article	IF	CITATIONS
37	Thermal performance improvement based on the partial heating position of a heat sink. International Journal of Heat and Mass Transfer, 2018, 124, 752-760.	4.8	19
38	Fabrication of micro-patterned aluminum surfaces for low ice adhesion strength. Applied Surface Science, 2018, 440, 643-650.	6.1	24
39	Fabrication of three-dimensional porous carbon scaffolds with tunable pore sizes for effective cell confinement. Carbon, 2018, 130, 814-821.	10.3	12
40	Defrosting behavior and performance on vertical plate for surfaces of varying wettability. International Journal of Heat and Mass Transfer, 2018, 120, 481-489.	4.8	20
41	Synthesis of cross-linked protein-metal hybrid nanoflowers and its application in repeated batch decolorization of synthetic dyes. Journal of Hazardous Materials, 2018, 347, 442-450.	12.4	145
42	Flexible elastomer patch with vertical silicon nanoneedles for intracellular and intratissue nanoinjection of biomolecules. Science Advances, 2018, 4, eaau6972.	10.3	39
43	Slippery Materials: Threeâ€Dimensionally Programmed Slippery Wrinkles with High Stretchability for Tunable Functionality of Icephobicity and Effective Water Harvesting (Adv. Mater. Interfaces 21/2018). Advanced Materials Interfaces, 2018, 5, 1870104.	3.7	0
44	Water-repellent Hybrid Nanowire and Micro-scale Denticle Structures on Flexible Substrates of Effective Air Retention. Scientific Reports, 2018, 8, 16631.	3.3	5
45	Genome-scale analysis of syngas fermenting acetogenic bacteria reveals the translational regulation for its autotrophic growth. BMC Genomics, 2018, 19, 837.	2.8	36
46	Genome-scale analysis of <i>Acetobacterium bakii</i> reveals the cold adaptation of psychrotolerant acetogens by post-transcriptional regulation. Rna, 2018, 24, 1839-1855.	3.5	10
47	Insights into Cell-Free Conversion of CO ₂ to Chemicals by a Multienzyme Cascade Reaction. ACS Catalysis, 2018, 8, 11085-11093.	11.2	87
48	Threeâ€Dimensionally Programmed Slippery Wrinkles with High Stretchability for Tunable Functionality of Icephobicity and Effective Water Harvesting. Advanced Materials Interfaces, 2018, 5, 1800980.	3.7	18
49	Quantitative analysis of anti-freezing characteristics of superhydrophobic surfaces according to initial ice nuclei formation time and freezing propagation velocity. International Journal of Heat and Mass Transfer, 2018, 126, 109-117.	4.8	21
50	Frosting and defrosting behavior of slippery surfaces and utilization of mechanical vibration to enhance defrosting performance. International Journal of Heat and Mass Transfer, 2018, 125, 858-865.	4.8	27
51	Minimizing thermal interference effects of multiple heat sources for effective cooling of power conversion electronics. Energy Conversion and Management, 2018, 174, 218-226.	9.2	13
52	Modeling of frost layer growth considering frost porosity. International Journal of Heat and Mass Transfer, 2018, 126, 980-988.	4.8	37
53	Facile Fabrication of Superomniphobic Polymer Hierarchical Structures for Directional Droplet Movement. ACS Applied Materials & Interfaces, 2017, 9, 9213-9220.	8.0	24
54	Frosting characteristics on hydrophobic and superhydrophobic surfaces: A review. Energy Conversion and Management, 2017, 138, 1-11.	9.2	120

#	Article	IF	CITATIONS
55	Three-Dimensional Hetero-Integration of Faceted GaN on Si Pillars for Efficient Light Energy Conversion Devices. ACS Nano, 2017, 11, 6853-6859.	14.6	7
56	BiVO ₄ /WO ₃ /SnO ₂ Double-Heterojunction Photoanode with Enhanced Charge Separation and Visible-Transparency for Bias-Free Solar Water-Splitting with a Perovskite Solar Cell. ACS Applied Materials & Interfaces, 2017, 9, 1479-1487.	8.0	158
57	Determination of the Genome and Primary Transcriptome of Syngas Fermenting Eubacterium limosum ATCCÂ8486. Scientific Reports, 2017, 7, 13694.	3.3	44
58	Fabrication of three-dimensional metal-graphene network phase change composite for high thermal conductivity and suppressed subcooling phenomena. Energy Conversion and Management, 2017, 149, 608-615.	9.2	34
59	Frost behavior of a louvered fin heat exchanger with vortex-generating fins. International Journal of Heat and Mass Transfer, 2017, 114, 590-596.	4.8	13
60	Stochastic approach to the anti-freezing behaviors of superhydrophobic surfaces. International Journal of Heat and Mass Transfer, 2017, 106, 841-846.	4.8	34
61	Numerical characterization of micro-cell UO2Mo pellet for enhanced thermal performance. Journal of Nuclear Materials, 2016, 477, 88-94.	2.7	18
62	Microscopic observation of frost behaviors at the early stage of frost formation on hydrophobic surfaces. International Journal of Heat and Mass Transfer, 2016, 97, 861-867.	4.8	33
63	A novel louvered fin design to enhance thermal and drainage performances during periodic frosting/defrosting conditions. Energy Conversion and Management, 2016, 110, 494-500.	9.2	45
64	Enhancement of photo-thermal conversion using gold nanofluids with different particle sizes. Energy Conversion and Management, 2016, 112, 21-30.	9.2	128
65	Frosting behaviors and thermal performance of louvered fins with unequal louver pitch. International Journal of Heat and Mass Transfer, 2016, 95, 499-505.	4.8	35
66	Optimum hub height of a wind turbine for maximizing annual net profit. Energy Conversion and Management, 2015, 100, 90-96.	9.2	34
67	Rotation characteristic and granular temperature analysis in a bubbling fluidized bed of binary particles. Particuology, 2015, 18, 76-88.	3.6	8
68	Direct growth of cerium oxide nanorods on diverse substrates for superhydrophobicity and corrosion resistance. Applied Surface Science, 2015, 340, 96-101.	6.1	74
69	Correlation of cross-cut cylindrical heat sink to improve the orientation effect of LED light bulbs. International Journal of Heat and Mass Transfer, 2015, 84, 821-826.	4.8	34
70	Local frost behaviors of a scaled-up louvered fin heat exchanger. International Journal of Heat and Mass Transfer, 2015, 89, 1127-1134.	4.8	19
71	Experimental investigation of frost retardation for superhydrophobic surface using a luminance meter. International Journal of Heat and Mass Transfer, 2015, 87, 491-496.	4.8	36
72	Fabrication of nanowire electronics on nonconventional substrates by water-assisted transfer printing method. Proceedings of SPIE, 2015, , .	0.8	0

#	Article	IF	CITATIONS
73	Granular temperature and rotational characteristic analysis of a gas–solid bubbling fluidized bed under different gravities using discrete hard sphere model. Powder Technology, 2015, 271, 35-48.	4.2	18
74	Thermal performance of microchannel heat exchangers according to the design parameters under the frosting conditions. International Journal of Heat and Mass Transfer, 2014, 71, 626-632.	4.8	42
75	Transfer Printing Methods for Flexible Thin Film Solar Cells: Basic Concepts and Working Principles. ACS Nano, 2014, 8, 8746-8756.	14.6	89
76	Electroassisted Transfer of Vertical Silicon Wire Arrays Using a Sacrificial Porous Silicon Layer. Nano Letters, 2013, 13, 4362-4368.	9.1	33
77	Local frosting behavior of a plated-fin and tube heat exchanger according to the refrigerant flow direction and surface treatment. International Journal of Heat and Mass Transfer, 2013, 64, 751-758.	4.8	34
78	Codoping titanium dioxide nanowires with tungsten and carbon for enhanced photoelectrochemical performance. Nature Communications, 2013, 4, 1723.	12.8	249
79	Peel-and-Stick: Fabricating Thin Film Solar Cell on Universal Substrates. Scientific Reports, 2012, 2, 1000.	3.3	66
80	Shrinking and Growing: Grain Boundary Density Reduction for Efficient Polysilicon Thin-Film Solar Cells. Nano Letters, 2012, 12, 6485-6491.	9.1	24
81	Thermal conductivity in porous silicon nanowire arrays. Nanoscale Research Letters, 2012, 7, 554.	5.7	64
82	Fabrication of Flexible and Vertical Silicon Nanowire Electronics. Nano Letters, 2012, 12, 3339-3343.	9.1	107
83	Hybrid Si Microwire and Planar Solar Cells: Passivation and Characterization. Nano Letters, 2011, 11, 2704-2708.	9.1	151
84	Branched TiO ₂ Nanorods for Photoelectrochemical Hydrogen Production. Nano Letters, 2011, 11, 4978-4984.	9.1	843
85	Fabrication of Nanowire Electronics on Nonconventional Substrates by Water-Assisted Transfer Printing Method. Nano Letters, 2011, 11, 3435-3439.	9.1	98
86	Vertical Transfer of Uniform Silicon Nanowire Arrays via Crack Formation. Nano Letters, 2011, 11, 1300-1305.	9.1	73
87	Methane oxidation over catalytic copper oxides nanowires. Proceedings of the Combustion Institute, 2011, 33, 3169-3175.	3.9	42
88	Fabricating nanowire devices on diverse substrates by simple transfer-printing methods. Proceedings of the United States of America, 2010, 107, 9950-9955.	7.1	123
89	Direct Growth of Nanowire Logic Gates and Photovoltaic Devices. Nano Letters, 2010, 10, 1050-1054.	9.1	29
90	Orientation-Controlled Alignment of Axially Modulated pn Silicon Nanowires. Nano Letters, 2010, 10, 5116-5122.	9.1	39

6

#	Article	IF	CITATIONS
91	Probing Flow Velocity with Silicon Nanowire Sensors. Nano Letters, 2009, 9, 1984-1988.	9.1	72
92	Single and Tandem Axial <i>p-i-n</i> Nanowire Photovoltaic Devices. Nano Letters, 2008, 8, 3456-3460.	9.1	401
93	Numerical Characterization and Optimization of the Microfluidics for Nanowire Biosensors. Nano Letters, 2008, 8, 3233-3237.	9.1	60
94	3-D Numerical Simulation of Contact Angle Hysteresis for Slug Flow in Microchannel. , 2007, , 955.		0
95	Compact Model of Slug Flow in Microchannels. , 2007, , .		1